

Comparison of 3D MRI with high sampling efficiency and 2D multiplanar MRI for contouring in cervix cancer brachytherapy

Primož Petric¹, Robert Hudej¹, Peter Rogelj², Mateja Blas³, Barbara Segedin¹, Helena Barbara Zobec Logar¹, Johannes Carl Athanasios Dimopoulos⁴

¹ Department of Radiotherapy, Institute of Oncology Ljubljana, Ljubljana, Slovenia

² University of Primorska, Faculty of Mathematics, Natural Sciences and Information Technologies, Koper, Slovenia

³ Institute of Oncology Ljubljana, Research Sector, Unit for Biostatistics, Ljubljana, Slovenia

⁴ Metropolitan Hospital, Department of Radiotherapy, Athens, Greece

Radiol Oncol 2012; 46(3): 242-251.

Received 1 January 2012

Accepted 17 February 2012

Correspondence to: Primož Petrič, MD, MSc, Department of Radiotherapy, Institute of Oncology Ljubljana, Zaloška 2, 1000 Ljubljana, Slovenia. Phone: +386 1 5879 206; Fax: +386 1 5879 400; E-mail: ppetric@onko-i.si

Disclosure: No potential conflicts of interest were disclosed.

Background. MRI sequences with short scanning times may improve accessibility of image guided adaptive brachytherapy (IGABT) of cervix cancer. We assessed the value of 3D MRI for contouring by comparing it to 2D multi-planar MRI.

Patients and methods. In 14 patients, 2D and 3D pelvic MRI were obtained at IGABT. High risk clinical target volume (HR CTV) was delineated by 2 experienced radiation oncologists, using the conventional (2D MRI-based) and test (3D MRI-based) approach. The value of 3D MRI for contouring was evaluated by using the inter-approach and inter-observer analysis of volumetric and topographic contouring uncertainties. To assess the magnitude of deviation from the conventional approach when using the test approach, the inter-approach analysis of contouring uncertainties was carried out for both observers. In addition, to assess reliability of 3D MRI for contouring, the impact of contouring approach on the magnitude of inter-observer delineation uncertainties was analysed.

Results. No approach- or observer - specific differences in HR CTV sizes, volume overlap, or distances between contours were identified. When averaged over all delineated slices, the distances between contours in the inter-approach analysis were 2.6 (Standard deviation (SD) 0.4) mm and 2.8 (0.7) mm for observers 1 and 2, respectively. The magnitude of topographic and volumetric inter-observer contouring uncertainties, as obtained on the conventional approach, was maintained on the test approach. This variation was comparable to the inter-approach uncertainties with distances between contours of 3.1 (SD 0.8) and 3.0 (SD 0.7) mm on conventional and test approach, respectively. Variation was most pronounced at caudal HR CTV levels in both approaches and observers.

Conclusions. 3D MRI could potentially replace multiplanar 2D MRI in cervix cancer IGABT, shortening the overall MRI scanning time and facilitating the contouring process, thus making this treatment method more widely employed.

Key words: cervix cancer; brachytherapy; contouring; MRI

Introduction

Image guided adaptive brachytherapy (IGABT) enables individualized irradiation, applying high doses to the target volume while respecting organs at risk (OAR) dose constraints.^{1,2} Accurate contouring of these regions is a precondition for treatment

success and consistent reporting in brachytherapy as well as in external beam irradiation.³ Various imaging modalities have been employed in gynaecological IGABT.⁴⁻²³ T2 weighted fast spin echo (T2w FSE) MRI currently represents the modality of choice due to its high soft tissue depiction quality.¹⁶⁻²⁸ Favourable reports on diagnostic and

dosimetric outcome of MRI based approach are reflected in encouraging clinical results.^{18-24,29,30}

However, limited access to MRI precludes its widespread adoption in this field. Until the role of low cost modalities (CT and US) is systematically evaluated, implementation of high resolution MRI sequences with short scanning times may make IGABT available to a wider population of patients. Currently, assessment of multiplanar post-insertion 2D T2w FSE MRI is required for accurate contouring.^{1,2,27} However, majority of treatment planning systems (TPS) do not enable import of non-resampled images in multiple planes. Classically, only (para)transverse images are imported and used for delineation, while other planes are resampled by the TPS from the (para)transverse set. Due to the slice thickness of 3-5 mm, the resampled images have poor resolution and are not useful for evaluation of patho-anatomical structures (Figure 1A). Non-resampled high-resolution (para)sagittal and (para)coronal 2D MR images have to be obtained in addition. As a result, 2D multiplanar MRI is characterized by long scanning time and the need for a separate DICOM-viewer to integrate findings from different planes during contouring.^{1,2,27,28} This approach is currently used at the Institute of Oncology Ljubljana. In addition, a 3D T2w FSE sequence with high sampling efficiency, 1 mm isotropic voxel size and large field of view (SPACE) is obtained at our department (Figure 1B). 3D MRI is co-registered with 2D para-transverse images in the TPS to reduce applicator reconstruction uncertainties.³¹ Due to the small voxel size, high resolution images in multiple planes can be resampled by the TPS from the 3D data-set (Figure 1C).

The aim of our study was to assess whether the 3D SPACE sequence could potentially replace multiplanar 2D MRI for contouring of high risk clinical target volume (HR CTV). By omitting multiplanar 2D MRI, the scanning time would be shortened. In addition, utilizing high-resolution images, resampled in multiple planes from the 3D data-set by the TPS, the separate DICOM viewer would no longer be required and fusion of multiple image series with its inherent uncertainties could be avoided.

Patients and methods

The value of 3D MRI for contouring was evaluated by using the inter-approach and inter-observer analysis of volumetric and topographic contouring uncertainties. In addition, to assess reliability of 3D MRI for contouring, the impact of contouring ap-

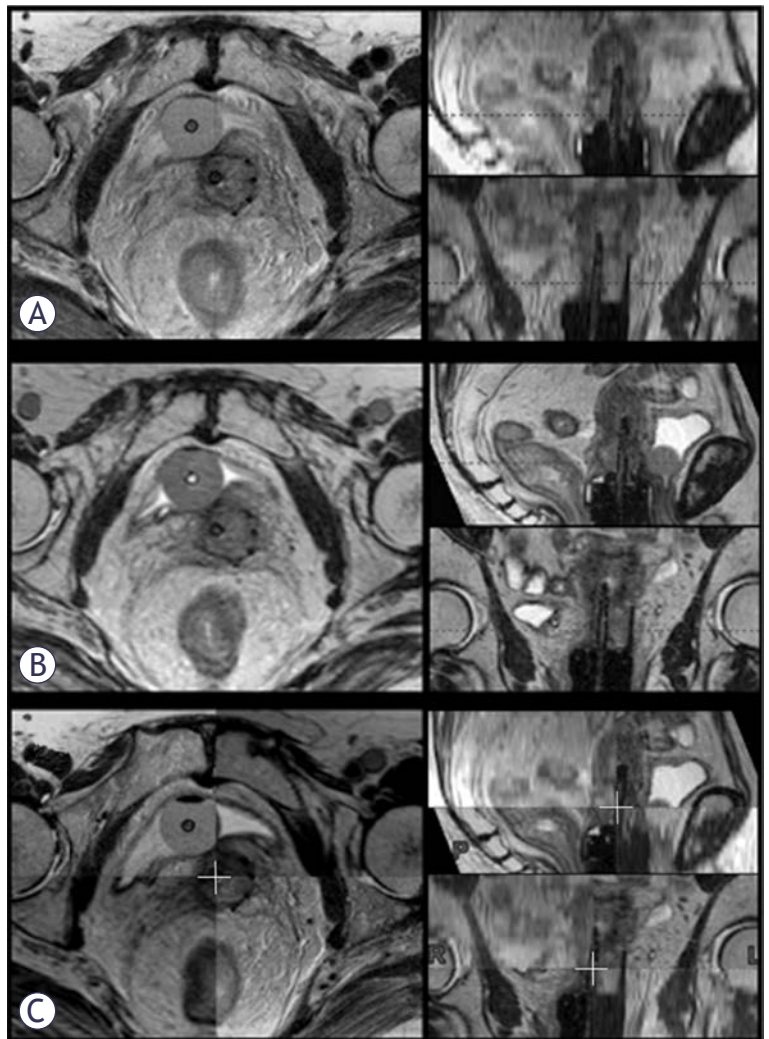


FIGURE 1. Post-insertion pelvic MRI. (A) Para-transverse 2D T2w FSE MR images were imported into the TPS (left). Para-sagittal and -coronal images were resampled from this data-set (right): due to the 3.9 mm slice thickness, their resolution is poor. (B) 3D MRI data-set was imported into the TPS. High resolution para-transverse (left), -sagittal and -coronal images (right) were resampled due to an isotropic voxel size of 1 mm. (C) Co-registration of the 2D para-transverse and 3D MRI data-sets.

proach on the magnitude of inter-observer delineation uncertainties was analysed.

To assess the magnitude of deviation from the conventional approach when using the test approach, the inter-approach analysis of contouring uncertainties was performed for both observers.

The study was carried out according to the Helsinki Declaration.

Patients and tumours

Fourteen consecutive patients with biopsy proven cervix cancer (8 FIGO stage IIB and 6 stage IIIB), treated at our department with radical MRI-based

IGABT between December 2006 and September 2007, were included. Mean tumour width, thickness and height, measured from the MRI at diagnosis, were 51 (Standard deviation (SD 11), 41 (SD 10) and 45 (SD 16) mm, respectively. Treatment consisted of 3D conformal CT-based external beam radiotherapy +/- concurrent chemotherapy, followed by 2 fractions of MRI-based pulsed dose rate IGABT. Details of our treatment strategy were presented elsewhere.³² First IGABT fraction from each case was used for analysis.

Post-insertion MRI and image registration

Planning MRI was obtained after applicator insertion at a 1.5 T scanner (Siemens Magnetom Avanto© 2006, Siemens AG, Erlangen, Germany), using a pelvic surface phased-array coil. 2D T2w FSE images (slice thickness 3 mm, interslice gap 0.9 mm, in-plane pixel size 0.6 × 0.6 mm, field of view 20 × 20 cm, matrix size 288 × 320, echo time 98 ms, repetition time 5700 ms, flip angle 150°, acquisition time ≈12 minutes), were obtained in para-transverse (perpendicular to cervical canal), para-coronal and para-sagittal (parallel to cervical canal) plane. In addition, 3D isotropic T2w FSE sequence with high sampling efficiency (SPACE, a vendor-specific sequence) was performed (176 slices, isotropic voxel size of 1 mm, field of view 40 × 40 cm, matrix size 384 × 386, echo time 131 ms, repetition time 1500 ms, flip angle 150°, acquisition time ≈7 minutes). Para-transverse 2D images and 3D data set were transferred to the TPS (Brachyvision, version 8.5, Copyright© 1996-2008 Varian Medical Systems Inc., Palo Alto, USA) and co-registered, using shared DICOM coordinates. Manual registration corrections were applied where patient movement occurred between sequences. From the 3D data-set, para-transverse, para-coronal and para-sagittal images were resampled within the TPS to match the slice thickness and acquisition planes of the 2D images (Figure 1C).

Contouring

HR CTV was outlined independently by 2 experienced radiation oncologists, respecting the GEC-ESTRO recommendations, using two different approaches.¹ (1) *Conventional approach*: contouring on non-resampled para-transverse 2D MRI; during delineation, non-resampled para-sagittal and para-coronal 2D images were available on a separate DICOM viewer to assess topographical relations between the target, applicator and normal

anatomical structures in 3 dimensions. This information was taken into account and integrated on para-transverse images in the TPS, where contouring was performed. (2) *Test approach*: contouring on para-transverse images, resampled from the 3D MRI; resampled high resolution para-sagittal and para-coronal images were available in the TPS contouring windows (Figure 1B), enabling direct incorporation of spatial information on pathological structures and interactive assessment of contours in all planes, without the use of an additional DICOM viewer. Contours, obtained in this study, were used for the purpose of analysis only, not for actual treatment. The interval between conventional and test contouring was at least one month.

Volumetric and topographic analysis

Using a dedicated software tool (Contour Analysis Tool – CAT, version 2), developed at our departments, inter-approach (intra-observer) and inter-observer contouring variation was assessed for each observer and approach, respectively. In volumetric analysis, HR CTV sizes were compared. In addition, volumetric conformity index (VCI) was computed for pairs of HR CTVs as the ratio between the common and encompassing volume³³, and compared within the inter-approach and inter-observer analysis. The common volume is defined as the intersection of two contoured volumes, while the encompassing volume is their union. In topographic analysis of inter-approach variations, the shortest 2D distance between conventional and test contour was calculated for each contour point on each slice for both observers. In inter-observer assessment, corresponding distances between delineations of the two observers were measured for both approaches. In order to identify eventual dependence of the variation magnitude on cranio-caudal level of the contoured volume, the analysis was carried out for all slices and, in addition, for the following HR CTV levels: (1) caudal-most two, (2) mid-level, and (3) cranial-most two slices.

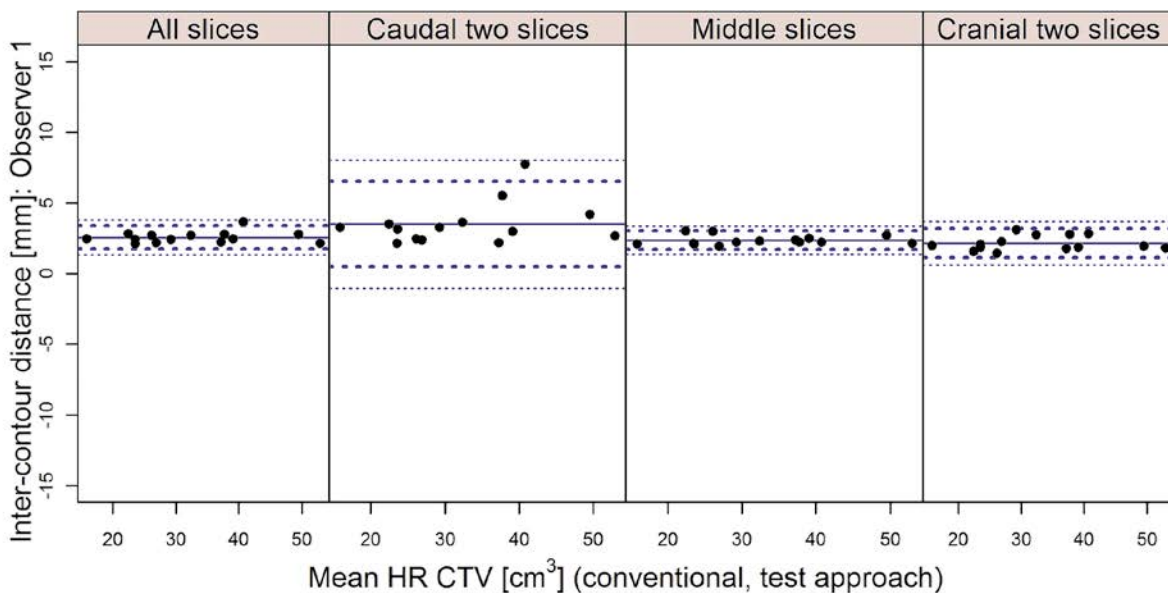
Statistical analysis

Continuous numerical variables were presented as mean values and standard deviations. Inter-approach and inter-observer variation was assessed by calculating Bland-Altman limits of agreement^{34,35}, and Lin's concordance correlation coefficient.^{36,37} We used the bootstrap method to obtain a more reliable 95% confidence interval for the cor-

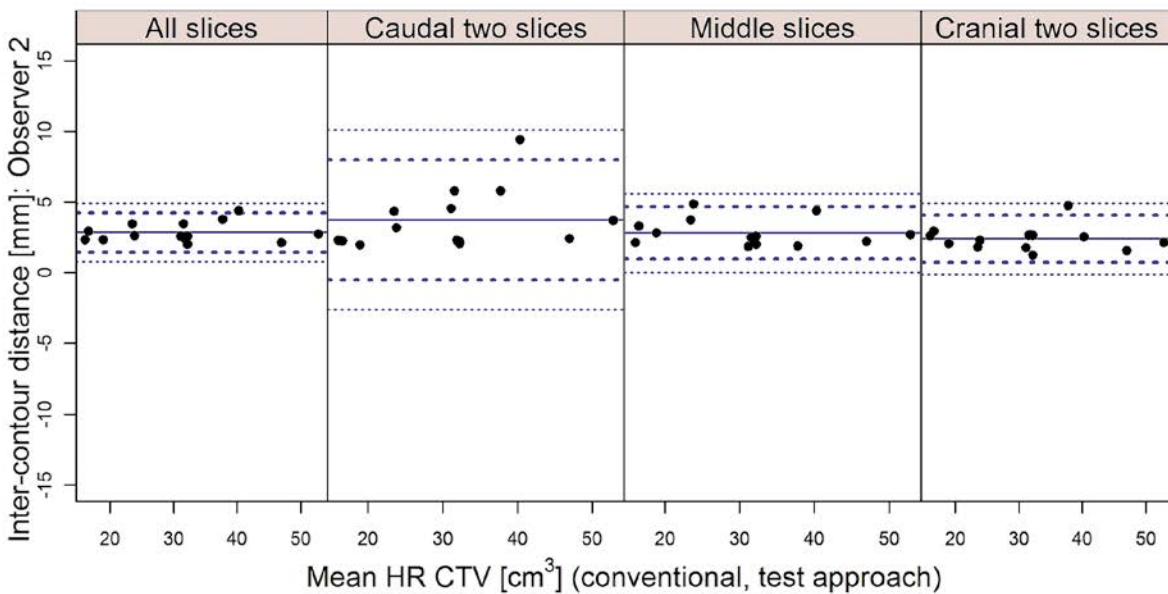
TABLE 1. Inter-approach and inter-observer differences in HR CTV sizes

	Diff. in HR CTV [cm ³] (mean (SD))	Limits of agreement (mean +/- 2SD) [cm ³]	95% CI [cm ³]	CCC	95% boot CI
Inter-approach analysis					
Observer 1	-1.2 (2.3)	-5.8, 3.4	-8.0, 5.7	0.97	0.94, 0.99
Observer 2	1.4 (2.8)	-4.3, 7.1	-7.1, 10.0	0.96	0.88, 0.99
Inter-observer analysis					
Conventional approach	2.8 (4.5)	-6.2, 11.9	-10.8, 16.4	0.87	0.75, 0.96
Test approach	0.3 (4.5)	-8.7, 9.2	-13.2, 13.7	0.91	0.84, 0.96

SD = standard deviation of differences; 95% CI = limits of 95% confidence interval for lower and upper limit; CCC = Lin's concordance correlation coefficient; 95% boot CI = 95% bootstrap confidence interval for CCC



(A)



(B)

FIGURE 2. Bland-Altman inter-approach analysis of the distances between contours for observer 1 (A) and 2 (B) and for different levels of the contoured volume (all, caudal two, middle and cranial two slices). Full circles: mean values (mm) of the individual distances. Thick dotted lines: limits of agreement (mean ± 2 standard deviations). Thin dotted lines: 95% confidence limits.

relation coefficient. All analyses and graphs were performed using a statistical program R (version 2.11.1., R Foundation for Statistical Computing, Vienna, Austria).

Results

No approach- or observer - specific differences in HR CTV sizes, VCI, or distances between contours were identified. The magnitude of topographic and volumetric inter-observer contouring uncertainties, as obtained on the conventional approach, was maintained on the test approach. This variation was comparable to the inter-approach uncertainties from both observers. Variation was most pronounced at caudal HR CTV levels in both approaches and observers. Detailed results of our analysis are presented below.

Using the conventional approach, mean HR CTVs of 32 (Standard deviation (SD) 10.5) cm³ and 31.8 (SD 10.8) cm³ were obtained for observer 1 and 2, respectively. Using the test approach, the respective HR CTV sizes were 33.2 (SD 11.0) cm³ and 30.4 (SD 11.2) cm³.

Using the inter-approach Bland-Altman analysis, high agreement in HR CTV sizes was found for both observers (Table 1). A favourable mean VCI of 0.8 (SD 0.03) and 0.79 (SD 0.04) was obtained for observer 1 and 2, respectively. The results of the Bland-Altman analysis of the inter-approach distances between contours were comparable for both observers and are presented in Table 2 and Figure 2. When averaged over all slices of the HR CTV, mean inter-approach distances were 2.6 mm (SD 0.4 mm) for observer 1 and 2.8 mm (SD 0.7 mm) for observer 2. Inter-approach contouring variation was most pronounced at the caudal level of the HR CTV (observer 1: 3.5 mm, SD 1.5 mm; observer 2: 3.7 mm; SD 2.1 mm). At the mid and cranial levels of the HR CTV, the inter-approach distances between contours were smaller (Table 2, Figure 2).

On the inter-observer analysis, high agreement in HR CTV sizes was found for both approaches (Table 1). Favourable mean VCI on conventional approach of 0.76 (SD 0.05) was maintained on test approach (mean VCI: 0.75; SD 0.05). The results of the Bland-Altman analysis of the inter-observer distances between contours were comparable for both approaches and are presented in Table 2 and Figure 3. When averaged over all slices of the HR CTV, mean inter-observer distances between contours of 3.1 mm (SD 0.8 mm) were found on conventional and 3.0 mm (SD 0.7 mm) on test ap-

proach. Similar to the inter-approach analysis, highest inter-observer distances were obtained at the caudal level of the HR CTV on the inter-observer assessment and were comparable for both contouring approaches (conventional: 5.4 mm, SD 3.1 mm; test: 4.4 mm, SD 3.0 mm). At the mid and cranial levels of the HR CTV, the inter-observer distances were smaller (Table 2, Figure 3).

Discussion

The dose conformity in IGABT exceeds any other radiotherapy modality and even minimal contouring variation can result in significant uncertainties of optimized dose distribution.³⁷ This may have important clinical consequences and compromise treatment recording and reporting, undermining overall IGABT efficacy. One of the potential sources of systematic contouring variations is the choice of imaging modality.

High resolution 3D T2w FSE isotropic MRI with high sampling efficiency, small voxel size, large field of view and sufficient signal to noise ratio was introduced for diagnostic imaging of the pelvis and other anatomical regions, potentially improving the diagnostic possibilities of MRI.³⁸⁻⁴⁶ Nevertheless, it seems that further improvements of 3D MRI are required before it could be considered as a replacement for 2D multiplanar imaging in local staging.^{38,40} As far as imaging for gynaecological IGABT treatment planning is concerned, 2D T2w FSE multi-planar MRI is currently considered the modality of choice.^{1,2} Results of the MRI-based IGABT have been published by several groups, demonstrating improved chance of cure and reduced morbidity rates when compared to conventional radiography-based method.^{20-23,47} Nevertheless, in spite of these favourable reports, widespread utilization of MRI and IGABT remains impeded by limited resources.⁴⁸⁻⁵⁰ The innovative approach to 3D MRI-based contouring, evaluated in our study, may make IGABT more easily employed. By omitting post-insertion multi-planar 2D MRI and by using 3D SPACE sequence both for applicator reconstruction and contouring, the MRI scanning time was reduced from approximately 19 to 7 minutes in our study. The achieved reduction is comparable to other strategies that could be proposed to improve IGABT availability (i.e. combination of MRI for the first application and CT, ultrasound or radiography for subsequent application(s)). Importantly, by applying a single sequence, uncertainties due to eventual patient mo-

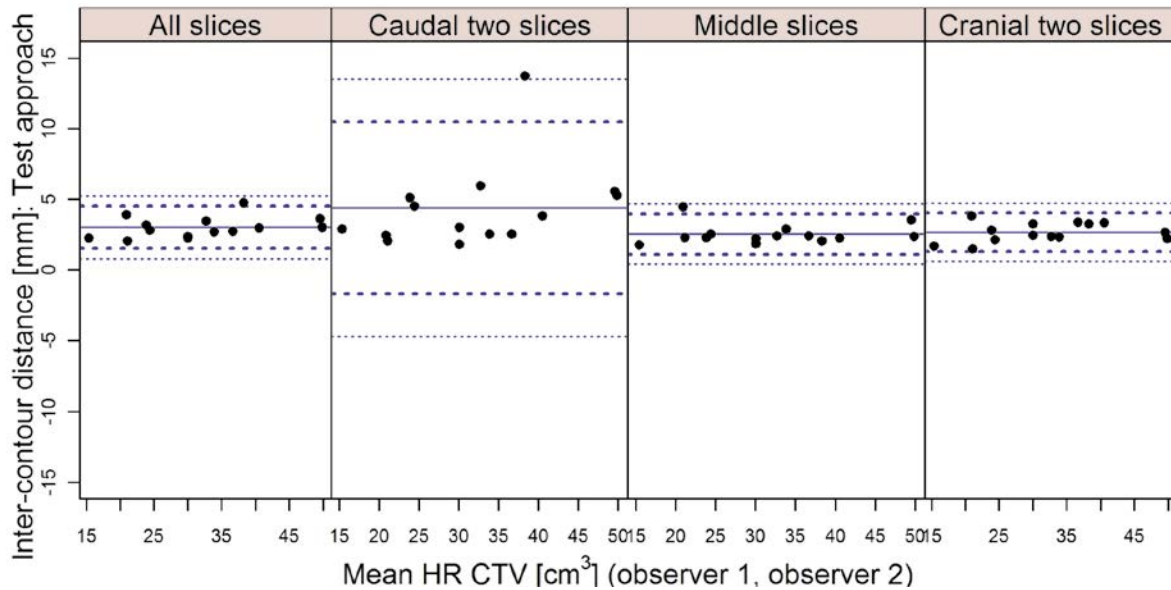
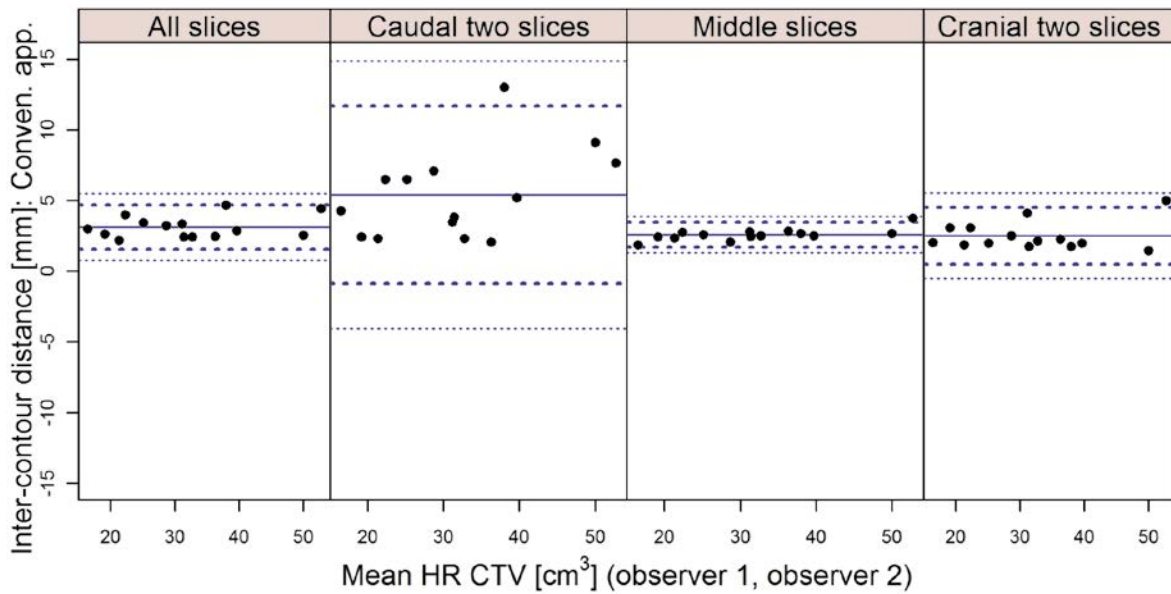


FIGURE 3. Bland-Altman inter-observer analysis of the distances between contours for conventional (A) and test (B) approach and for different levels of the contoured volume (all, caudal two, middle and cranial two slices). Full circles: mean values (mm) of the individual distances. Thick dotted lines: limits of agreement (mean \pm 2 standard deviations). Thin dotted lines: 95% confidence limits.

tion between sequences were reduced. However, the introduction of a new imaging approach could result in sequence-specific observer's interpretation of findings and systematic deviations from our standard technique. No such deviations could be found in our study. In addition, no observer-specific deviations were identified and the magnitude of intra-observer uncertainties was comparable to inter-observer variation.

VCI is one of the commonly used measures of volumetric similarity between delineated objects. Poor agreement is indicated by a low VCI. As the

agreement increases, VCI approaches 1. Small differences in HR CTV sizes (Table 1) and favourable results on VCI, obtained in our study, indicate high level of volumetric agreement between the conventional and test delineations. An inter-approach VCI of around 0.8 compares favourably with results of similar studies both in the field of EBRT and BT.⁵¹⁻⁵⁷ In addition, high inter-observer VCI of the conventional 2D MRI approach was maintained for 3D MRI-based contouring. However, the sensitivity of VCI to contouring deviations increases with decreasing size of analysed volumes: contouring

TABLE 2. Inter-approach and inter-observer distances between contours at different cranio-caudal levels of the HR CTV

	Inter-contour distance [mm] (mean (SD))	Limits of agreement [mm]	95% CI [mm]
All slices			
Inter-approach analysis			
Observer 1	2.6 (0.4)	1.8, 3.4	1.3, 3.8
Observer 2	2.8 (0.7)	1.5, 4.2	0.8, 4.9
Inter-observer analysis			
Conventional approach	3.1 (0.8)	1.5, 4.7	0.8, 5.5
Test approach	3.0 (0.7)	1.5, 4.5	0.8, 5.2
Caudal two slices			
Inter-approach analysis			
Observer 1	3.5 (1.5)	0.5, 6.5	-1.0, 8.0
Observer 2	3.7 (2.1)	-0.5, 8.0	-2.6, 10.1
Inter-observer analysis			
Conventional approach	5.4 (3.1)	-0.9, 11.7	-4.0, 14.9
Test approach	4.4 (3.0)	-1.7, 10.5	-4.7, 13.5
Middle slices			
Inter-approach analysis			
Observer 1	2.4 (0.3)	1.7, 3.0	1.7, 3.3
Observer 2	2.8 (0.9)	0.9, 4.7	0.0, 5.6
Inter-observer analysis			
Conventional approach	2.6 (0.4)	1.7, 3.5	1.3, 3.9
Test approach	2.5 (0.7)	1.1, 4.0	0.4, 4.7
Cranial two slices			
Inter-approach analysis			
Observer 1	2.1 (0.5)	1.1, 3.2	0.6, 3.7
Observer 2	2.4 (0.8)	0.7, 4.1	-0.1, 4.9
Inter-observer analysis			
Conventional approach	2.5 (1.0)	0.5, 4.5	-0.5, 5.5
Test approach	2.7 (0.7)	1.3, 4.0	0.6, 4.7

SD = standard deviation of differences; 95% CI = limits of 95% confidence interval for lower and upper limit.

deviation of a given absolute magnitude will be reflected in a more favourable VCI when analysing large, compared to small volumes. This makes direct comparisons of results between EBRT (typically large volumes) and BT (typically small volumes) studies challenging. In addition, the possibility to directly compare studies is limited due to differences in formalisms applied and the number of observers/cases analysed.⁵¹⁻⁵³ Nevertheless; our results indicate that the implementation of 3D MRI for contouring introduced no volumetric uncertainties when compared to the conventional approach.

VCI gives no information on the absolute magnitude of contouring variations and their topogra-

phy. However, brachytherapy is characterized by an inhomogeneous dose distribution with a steep dose gradient. Consequently, the magnitude and topography of contouring uncertainties have a direct impact on treatment. In our study, quantitative assessment of variability revealed mean distances of up to 2.8 (SD 0.9) mm and 2.7 (SD 0.7) mm between analysed pairs of contours for the middle and cranial parts of the HR CTV, respectively. In caudal parts of the contoured volumes, mean inter-approach and inter-observer distances between delineations of up to 3.7 (SD 2.1) and 5.4 (SD 3.1) mm, respectively, were found (Table 2, Figures 2, 3). Therefore, higher variability was present in those

parts of the HR CTV, which are typically located in the close proximity of the ring source-channel. It has to be noted that up to approximately 4% deviation of commonly reported DVH parameters for the HR CTV can be expected per mm relative displacement of the contours with respect to the applicator.⁵⁸ In addition, relatively large standard deviations of inter-contour distances reflect a considerable spread of individual values, in particular in the caudal regions of the HR CTV (Table 2, Figures 2, 3). Assessment of the effects of these variations on the commonly evaluated dose-volume parameters was not a subject of our investigation and will deserve special attention in the future. Contouring variation should be considered as one of the most important sources of uncertainties in IGABT.

Due to a 1 mm isotropic voxel size, 3D MRI allowed for a high-resolution image resampling in any plane within the TPS (Figure 1B). In this way, the need for an additional DICOM viewer during delineation could be omitted, reducing the infrastructural requirements of the department and facilitating contouring.

There are some limitations of our study. We evaluated the capability of 3D MRI to replace conventional 2D multi-planar MRI for delineation of HR CTV. The value of this approach for contouring of the gross tumour volume and intermediate risk CTV was not assessed. However, since the HR CTV is currently the most widely used volume for dose prescription and optimisation in IGABT, our results can be considered practically relevant.^{20,22,23,29} Next, since the inter-observer analysis was chosen to assess the inter-approach variations it could be argued that the number of observers (2) may be suboptimal and that the reported differences in inter-observer comparison could be attributed to the variability caused by particular case and not the observer. However, due to the specific expertise, required for the competence of a radiation oncologist in the field of cervix cancer IGABT, it is very challenging to obtain a higher number of observers for this purpose in a mono-institutional setting. Our results should be regarded as an indication of the value of the 3D MRI in gynaecological IGABT. However, further studies with higher number of observers may be required to confirm this. Finally, the SPACE sequence is vendor-specific. Before extrapolating the findings of our study to sequences from other vendors, additional work may be required.

It has to be noted that the pixel dimensions are larger on the para-transverse images, resampled from the 3D MRI (1 × 1 mm) when compared to

the conventional para-transverse 2D MRI (0.6 × 0.6 mm). This results in a lower resolution and image quality in the main contouring plane. Eventual improvements of the 3D MRI are expected to further enhance the capability to use these sequences for treatment planning. Nevertheless, our results demonstrate that the described limitation did not result in an increase of contouring uncertainties.

Potential impact of MRI characteristics on the applicator reconstruction uncertainties deserves special mention. The procedure of defining the source channels on the images is a crucial step in IGABT, since the dose calculation is based on the geometry of source positions.⁵⁹ Imaging with small slice thickness or the use of 3D sequences with isotropic voxel size has been recommended by the Gyn GEC-ESTRO working group to reduce the applicator reconstruction uncertainties. In addition, contouring and reconstruction should be performed preferably in the same image series to avoid fusion uncertainties.³⁰ 3D MRI, evaluated in our study, therefore seems particularly suitable for gynaecological IGABT. Due to a small voxel size it enables an accurate applicator reconstruction, while the uncertainties related to image registration and fusion (Figure 1C) are avoided by using a single sequence for contouring and applicator reconstruction.³¹

Conclusions

3D MRI-based contouring of HR CTV introduced no systematic deviations from the conventional 2D multi-planar MRI-based approach. By omitting multi-planar MRI and employing a single 3D sequence for treatment planning, total image acquisition time was shortened for more than 50 %, when compared to our conventional technique. In addition, uncertainties due to patient motion between sequences were reduced. The use of additional DICOM viewer was no longer required during delineation, facilitating the contouring process. By employing a single 3D MRI sequence with 1 mm isotropic voxel size both for contouring and applicator reconstruction, uncertainties of image registration and fusion are avoided and the applicator reconstruction facilitated. 3D MRI could be considered as an alternative to conventional 2D multi-planar MRI in cervix cancer IGABT, making this treatment method potentially more widely employed.

References

- Haie-Meder C, Pötter R, Van Limbergen E, Briot E, De Brabandere M, Dimopoulos J, et al. Recommendations from Gynaecological (GYN) GEC-ESTRO Working Group (I): concepts and terms in 3D image based 3D treatment planning in cervix cancer brachytherapy with emphasis on MRI assessment of GTV and CTV. *Radiother Oncol* 2005; **74**: 235-45.
- Pötter R, Haie-Meder C, Van Limbergen E, Barillot I, De Brabandere M, Dimopoulos J, et al. Recommendations from gynaecological (GYN) GEC-ESTRO Working Group: (II): concepts and terms of 3D imaging, radiation physics, radiobiology, and 3D dose volume parameters. *Radiother Oncol* 2006; **78**: 67-77.
- Yadav P, Ramasubramanian V, Paliwal BR. Feasibility study on effect and stability of adaptive radiotherapy on kilovoltage cone beam CT. *Radiol Oncol* 2011; **45**: 220-6.
- Mayr NA, Montebello JF, Sorosky JJ, Daugherty JS, Nguyen DL, Mardirossian G, et al. Brachytherapy management of the retroverted uterus using ultrasound-guided implant applicator placement. *Brachytherapy* 2005; **4**: 24-9.
- Sahinler I, Cepni I, Colpan D, Cepni K, Koksals S, Koca A, et al. Tandem application with transvaginal ultrasound guidance. *Int J Radiat Oncol Biol Phys* 2004; **59**: 190-6.
- Davidson MT, Yuen J, D'Souza D, Radwan JS, Hammond JA, Batchelar DL. Optimization of high-dose-rate cervix brachytherapy applicator placement: the benefits of intraoperative ultrasound guidance. *Brachytherapy* 2008; **7**: 248-53.
- Stock RG, Chan K, Terk M, Dewynngaert JK, Stone NN, Dottino P. A new technique for performing Syed -Neblett template interstitial implants for gynecologic malignancies using transrectal-ultrasound guidance. *Int J Radiat Oncol Biol Phys* 1997; **37**: 819-25.
- Weitmann HD, Knocke TH, Waldhäusl C, Pötter R. Ultrasound-guided interstitial Brachytherapy in the treatment of advanced vaginal recurrences from cervical and endometrial carcinoma. *Strahlenther Onkol* 2006; **182**: 86-95.
- Van Dyk S, Narayan K, Fisher R, Bernshaw D. Conformal brachytherapy planning for cervical cancer using transabdominal ultrasound. *Int J Radiat Oncol Biol Phys* 2009; **75**: 64-70.
- Datta NR, Srivastava A, Maria Das KJ, Gupta A, Rastogi N. Comparative assessment of doses to tumor, rectum, and bladder as evaluated by orthogonal radiographs vs. computer enhanced computed tomography-based intracavitary brachytherapy in cervical cancer. *Brachytherapy* 2006; **5**: 223-9.
- Shin KH, Kim TH, Cho JK, Kim JY, Park SY, Park SY, et al. CT-guided intracavitary radiotherapy for cervical cancer: Comparison of conventional point A plan with clinical target volume-based three-dimensional plan using dose volume parameters. *Int J Radiat Oncol Biol Phys* 2006; **64**: 197-204.
- Mai J, Rownd J, Erickson B. CT-guided high-dose-rate dose prescription for cervical carcinoma: the importance of uterine wall thickness. *Brachytherapy* 2002; **1**: 27-35.
- Weitmann HD, Pötter R, Waldhäusl C, Nechvile E, Kirisits C, Knocke TH. Pilot study in the treatment of endometrial carcinoma with 3D image-based high-dose-rate brachytherapy using modified Heyman Packing: clinical experience and dose-volume histogram analysis. *Int J Radiat Oncol Biol Phys* 2005; **62**: 468-78.
- Pelloski CE, Palmer M, Chronowski GM, Jhingran A, Horton J, Eifel PJ. Comparison between CT-based volumetric calculations and ICRU reference-point estimates of radiation doses delivered to bladder and rectum during intracavitary radiotherapy for cervical cancer. *Int J Radiat Oncol Biol Phys* 2005; **62**: 131-7.
- Sun LM, Huang EY, Ko SF, Wang CJ, Leung SW, Lin H, et al. Computer-tomography-assisted three-dimensional technique to assess rectal and bladder wall dose in intracavitary brachytherapy for uterine cervical cancer. *Radiother Oncol* 2004; **71**: 333-7.
- Schoeppel SL, Ellis JH, LaVigne ML, Schea RA, Roberts JA. Magnetic resonance imaging during intracavitary gynecologic brachytherapy. *Int J Radiat Oncol Biol Phys* 1992; **23**: 169-74.
- Tardivon AA, Kinkel K, Lartigau E, Masselot J, Gerbaulet AP, Vanel D. MR imaging during intracavitary brachytherapy of vaginal and cervical cancer: preliminary results. *Radiographics* 1996; **16**: 1363-70.
- Viswanathan AN, Cormack R, Holloway CL, Tanaka C, O'Farrell D, Devlin PM, et al. Magnetic resonance-guided interstitial therapy for vaginal recurrence of endometrial cancer. *Int J Radiat Oncol Biol Phys* 2006; **66**: 91-9.
- Wachter-Gerstner N, Wachter S, Reinstadler E, Fellner C, Knocke TH, Wambersie A, et al. Bladder and rectum dose defined from MRI based treatment planning for cervix cancer brachytherapy: comparison of dose-volume histograms for organ contours and organ wall, comparison with ICRU rectum and bladder reference point. *Radiother Oncol* 2003; **68**: 269-76.
- Pötter R, Dimopoulos J, Georg P, Lang S, Waldhäusl C, Wachter-Gerstner N, et al. Clinical impact of MRI assisted dose volume adaptation and dose escalation in brachytherapy of locally advanced cervix cancer. *Radiother Oncol* 2007; **83**: 148-55.
- Haie-Meder C, Chargari C, Rey A, Dumas I, Morice P, Magné N, et al. MRI-based low dose-rate brachytherapy experience in locally advanced cervical cancer patients initially treated by concomitant chemoradiotherapy. *Radiother Oncol* 2010; **96**: 161-5.
- De Brabandere M, Mousa AG, Nulens A, Swinnen A, Van Limbergen E. Potential of dose optimisation in MRI-based PDR brachytherapy of cervix carcinoma. *Radiother Oncol* 2008; **88**: 217-26.
- Lindegaard JC, Tanderup K, Nielsen SK, Haack S, Gelineck J. MRI-Guided 3D Optimization Significantly Improves DVH Parameters of Pulsed-Dose-Rate Brachytherapy in Locally Advanced Cervical Cancer. *Int J Radiat Oncol Biol Phys* 2008; **71**: 756-64.
- Boss EA, Barentsz JO, Massuger LF, Boonstra H. The role of MR imaging in invasive cervical carcinoma. *Eur Radiol* 2000; **10**: 256-70.
- Subak LL, Hricak H, Powell CB, Azizi L, Stern JL. Cervical carcinoma: computed tomography and magnetic resonance imaging for preoperative staging. *Obstet Gynecol* 1995; **86**: 43-50.
- Hricak H, Gatsonis C, Coakley FV, Snyder B, Reinhold C, Schwartz LH, et al. Early invasive cervical cancer: CT and MR imaging in preoperative evaluation - ACRIN/GOG comparative study of diagnostic performance and interobserver variability. *Radiology* 2007; **245**: 491-8.
- Mitchell DG, Snyder B, Coakley F, Reinhold C, Thomas G, Amendola M, et al. Early invasive cervical cancer: tumor delineation by magnetic resonance imaging, computed tomography, and clinical examination, verified by pathologic results, in the ACRIN 6651/GOG 183 Intergroup Study. *J Clin Oncol* 2006; **24**: 5687-94.
- Dimopoulos JC, Schard G, Berger D, Lang S, Goldner G, Helbich T, et al. Systematic evaluation of MRI findings in different stages of treatment of cervical cancer: potential of MRI on delineation of target, patho-anatomical structures and organs at risk. *Int J Radiat Oncol Biol Phys* 2006; **64**: 1380-8.
- Podobnik J, Kocijancic I, Kovac V, Sersa I. 3T MRI in evaluation of asbestos-related thoracic diseases - preliminary results. *Radiol Oncol* 2010; **44**: 92-6.
- Sofic A, Beslic S, Sehovic N, Caluk J, Sofic D. MRI in evaluation of perianal fistulae. *Radiol Oncol* 2010; **44**: 220-7.
- Dimopoulos JC, Schirl G, Baldinger A, Helbich TH, Pötter R, et al. MRI assessment of cervical cancer for adaptive radiotherapy. *Strahlenther Onkol* 2009; **185**: 282-7.
- Hellebust TP, Kirisits C, Berger D, Pérez-Calatayud J, De Brabandere M, De Leeuw A, et al. Recommendations from Gynaecological (GYN) GEC-ESTRO Working Group: Considerations and pitfalls in commissioning and applicator reconstruction in 3D image-based treatment planning of cervix cancer brachytherapy. *Radiother Oncol* 2010; **96**: 153-60.
- Petric P, Hudej R, Music M. MRI assisted cervix cancer brachytherapy pre-planning, based on insertion of the applicator in para-cervical anaesthesia: preliminary results of a prospective study. *J Contemp Brachyther* 2009; **1**: 163-9.
- Kouwenhoven E, Giezen M, Struikmans H. Measuring the similarity of target volume delineations independent of the number of observers. *Phys Med Biol* 2009; **54**: 2863-73.
- Bland JM, Altman DG. Statistical methods for assessing agreement between two methods of clinical measurements. *Lancet* 1986; **1**: 307-10.
- Bland JM, Altman DG. Measuring agreement in method comparison studies. *Stat Methods Med Res* 1999; **8**: 135-60.
- Lin LI. A concordance correlation coefficient to evaluate reproducibility. *Biometrics* 1989; **45**: 255-68.

38. Georg D, Kirisits C, Hillbrand M, Dimopoulos J, Pötter R. Image-guided radiotherapy for cervix cancer: high-tech external beam therapy versus high-tech brachytherapy. *Int J Radiat Oncol Biol Phys* 2008; **71**: 1272-8.
39. Lichy MP, Wietek BM, Mugler JP 3rd, Horger W, Menzel MI, Anastasiadis A, et al. Magnetic resonance imaging of the body trunk using a single-slab, 3-dimensional, T2-weighted turbo-spin-echo sequence with high sampling efficiency (SPACE) for high spatial resolution imaging: initial clinical experiences. *Invest Radiol* 2005; **40**: 754-60.
40. Fütterer JJ, Yakar D, Strijk SP, Barentsz JO. Preoperative 3T MR imaging of rectal cancer: local staging accuracy using a two-dimensional and three-dimensional T2-weighted turbo spin echo sequence. *Eur J Radiol* 2008; **65**: 66-71.
41. Kim H, Lim JS, Choi JY, Park J, Chung YE, Kim MJ, et al. Rectal cancer: comparison of accuracy of local-regional staging with two- and three-dimensional preoperative 3-T MR imaging. *Radiology* 2010; **254**: 485-92.
42. Rosenkrantz AB, Neil J, Kong X, Melamed J, Babb JS, Taneja SS, et al. Prostate cancer: Comparison of 3D T2-weighted with conventional 2D T2-weighted imaging for image quality and tumor detection. *AJR Am J Roentgenol* 2010; **194**: 446-52.
43. Arizono S, Isoda H, Maetani YS, Hirokawa Y, Shimada K, Nakamoto Y, et al. High-spatial-resolution three-dimensional MR cholangiography using a high-sampling-efficiency technique (SPACE) at 3T: Comparison with the conventional constant flip angle sequence in healthy volunteers. *J Magn Res Imaging* 2008; **28**: 685-90.
44. Arizono S, Isoda H, Maetani YS, Hirokawa Y, Shimada K, Nakamoto Y, et al. High spatial resolution 3D MR cholangiography with high sampling efficiency technique (SPACE): Comparison of 3 T vs. 1.5 T. *Eur J Radiol* 2010; **73**: 114-8.
45. Baumert B, Wörtler K, Steffinger D, Schmid GP, Schmidt GP, Reiser MF, Baur-Melnyk A. Assessment of the internal craniocervical ligaments with a new magnetic resonance imaging sequence: three dimensional turbo spin echo with variable flip-angle distribution (SPACE). *Magn Res Imaging* 2009; **27**: 954-60.
46. Young JY, Yoon YC, Kwon JW, Ahn JH, Choe BK. Diagnosis of internal derangement of the knee at 3.0 T MR imaging: 3D isotropic intermediate-weighted versus 2D sequences. *Radiology* 2009; **253**: 780-7.
47. Young JY, Yoon YC, Choi SH, Kwon JW, Yoo J, Choe BK. Three-dimensional isotropic shoulder MR arthrography for the diagnosis of labral lesions at 3.0 T. *Radiology* 2009; **250**: 498-505.
48. Gerbaulet A, Pötter R, Haie-Meder C. Cervix cancer. In: Gerbaulet A, Pötter R, Mazon JJ, Meertens H, Van Limbergen E, editors. *The GEC ESTRO handbook of brachytherapy*. Brussels: European Society of Therapeutic Radiology and Oncology; 2002. p 301-63.
49. Guedea F, Ellison T, Venselaar J, Borrás JM, Hoskin P, Poetter R, et al. Overview of brachytherapy resources in Europe: a survey of patterns of care study for brachytherapy in Europe. *Radiother Oncol* 2007; **82**: 50-4.
50. Guedea F, Venselaar J, Hoskin P, Hellebust TP, Peiffert D, Londres B, et al. Patterns of care for brachytherapy in Europe: updated results. *Radiother Oncol* 2010; **97**: 514-20.
51. Viswanathan AN, Erickson BA. Three-dimensional imaging in gynaecological brachytherapy: a survey of the American Brachytherapy Society. *Int J Radiat Oncol Biol Phys* 2010; **76**: 104-9.
52. Dimopoulos JC, De Vos V, Berger D, Dumas I, Kirisits C, Shenfield CB, et al. Inter-observer comparison of target delineation for MRI-assisted cervical cancer brachytherapy: application of the GYN GEC-ESTRO recommendations. *Radiother Oncol* 2009; **91**: 166-72.
53. Lang S, Nulens A, Briot E, Kirisits C, De Brabandere M, Dumas I, Dimopoulos J, et al. Intercomparison of treatment concepts for MR image assisted brachytherapy of cervical carcinoma based on GYN GEC-ESTRO recommendations. *Radiother Oncol* 2006; **78**: 185-93.
54. Petric P, Dimopoulos J, Kirisits C, Berger D, Hudej R, Pötter R. Inter- and intraobserver variation in HR-CTV contouring: Intercomparison of transverse and paratransverse image orientation in 3D-MRI assisted cervix cancer brachytherapy. *Radiother Oncol* 2008; **89**: 164-71.
55. Rasch C, Barillot I, Remeijer P, Touw A, van Herk M, Lebesque JV. Definition of the prostate in CT and MRI: a multiobserver study. *Int J Radiat Oncol Biol Phys* 1999; **43**: 57-66.
56. Struikmans H, Warlam-Rodenhuis C, Stam T, Stapper G, Tersteeg RJ, Bol GH, et al. Interobserver variability of clinical target volume delineation of glandular breast tissue and of boost volume in tangential breast irradiation. *Radiother Oncol* 2005; **76**: 293-9.
57. Hurkmans CW, Borger JH, Pieters BR, Russell NS, Jansen EP, Mijnheer BJ. Variability in target volume delineation on CT scans of the breast. *Int J Radiat Oncol Biol Phys* 2001; **50**: 1366-72.
58. Weiss E, Richter S, Krauss T, Metzeltin SI, Hille A, Pradier O, et al. Conformal radiotherapy planning of cervix carcinoma: differences in the delineation of target volume. A comparison between gynaecologic and radiation oncologists. *Radiother Oncol* 2003; **67**: 87-95.
59. Tanderup K, Hellebust TP, Lang S, Granfeldt J, Pötter R, Lindegaard JC, et al. Consequences of random and systematic reconstruction uncertainties in 3D image based brachytherapy in cervical cancer. *Radiother Oncol* 2008; **98**: 156-63.